Anal Bioanal Chem (2017) 409:589–606
DOI 10.1007/s00216-016-0029-4

RESEARCH PAPER

Quantitation of human milk proteins and their glycoforms using multiple reaction monitoring (MRM)

Jincui Huang[1,2] · Muchena J. Kailemia[1] · Elisha Goonatilleke[1] · Evan A. Parker[1] · Qiuting Hong[1,2] · Rocchina Sabia[3] · Jennifer T. Smilowitz[2,4] · J. Bruce German[2,4] · Carlito B. Lebrilla[1,2]

Received: 28 June 2016 / Revised: 26 September 2016 / Accepted: 11 October 2016 / Published online: 29 October 2016

Abstract Human milk plays a substantial role in the child growth, development and determines their nutritional and health status. Despite the importance of the proteins and glycoproteins in human milk, very little quantitative information especially on their site-specific glycosylation is known. As more functions of milk proteins and other components continue to emerge, their fine-detailed quantitative information is becoming a key factor in milk research efforts. The present work utilizes a sensitive label-free MRM method to quantify seven milk proteins (α-lactalbumin, lactoferrin, secretory immunoglobulin A, immunoglobulin G, immunoglobulin M, α1-antitrypsin, and lysozyme) using their unique peptides while at the same time, quantifying their site-specific N-glycosylation relative to the protein abundance. The method is highly reproducible, has low limit of quantitation, and accounts for differences in glycosylation due to variations in protein amounts. The method described here expands our knowledge about human milk proteins and provides vital details that could be used in monitoring the health of the infant and even the mother.

Keywords Human milk · MRM · Glycoproteomics · UPLC · Mass spectrometry

Published in the topical collection *Glycomics, Glycoproteomics and Allied Topics* with guest editors Yehia Mechref and David Muddiman.

Electronic supplementary material The online version of this article (doi:10.1007/s00216-016-0029-4) contains supplementary material, which is available to authorized users.

✉ Carlito B. Lebrilla
cblebrilla@ucdavis.edu

[1] Department of Chemistry, University of California, Davis, CA 95616, USA

[2] Foods for Health Institute, University of California, 1 Shields Ave, Davis, CA 95616, USA

[3] Department of Drug Chemistry and Technologies, University of Rome, Piazzale Aldo Moro 5, 00185 Rome, Italy

[4] Department of Food Science and Technology, University of California, 392 Old Davis Road, Davis, CA 95616, USA

Introduction

Human milk contains abundant biologically active components, including proteins, endogenous peptides, lipids, carbohydrates, and minerals, which contribute to the nutritional and physiological wellbeing of newborns [1–7]. Human milk proteins provide primary nutrients for the infant and also protect them against infections via antimicrobial and immunemodulatory activities that helps build immunity of the breast-fed infant [8, 9]. Accurate and sensitive quantitation of human milk proteins is expected to contribute to our understanding of the milk biogenesis and their benefits to the neonates.

The vast majority of human milk proteins are glycosylated. It has been reported that glycosylation helps to reduce the number of pathogenic infections and promotes the development of the intestinal epithelium [7, 10]. Glycosylation is a common but complicated protein post-translational modification (PTM). It plays key roles in many biological functions, such as stabilizing the glycoprotein structure, mediating cell signaling and cell–cell recognition events, and modulating microbial adhesion and invasion during infection [11–14].

α-Lactalbumin (α-Lact) is one of the most abundant proteins in milk. Proteolytic fragments of α-Lact have prebiotic properties useful in stimulating the growth of beneficial bacteria besides its well-known roles in lactose biosynthesis [15, 16]. Lactoferrin (LF) is a major glycoprotein in human milk

with several physiological functions including bacteriostatic, antiviral, and antibacterial [4, 7–9]. The dominant antibody in human milk, secretory immunoglobulin A (sIgA), has immunological properties and anti-pathogenic activities [17]. It is known that glycans on sIgA bind to pathogens that threaten the health of the newborns [18–20]. Besides sIgA, there are other immunoglobulins in human milk that are also glycosylated such as immunoglobulin G (IgG) and immunoglobulin M (IgM). α1-Antitrypsin (A1AT), with three N-glycosites, is present in human milk as a protease inhibitor. It is believed that A1AT can help limit protein digestion during early infancy when its concentration is relative high. As a result, A1AT can also facilitate the action of other bioactive proteins [21, 22]. Lysozyme (LZ), while not glycosylated, is another protective milk protein. It is an enzyme that breaks β1,4 bonds between GlcNAc residues, thus playing a key role in the defense of mucus membrane against infections [23].

Despite the numerous studies on milk proteins, nutritive and protective functions, their simultaneous quantitation has not been performed nor has the extent of their glycosylation level been fully characterized. The analytical methods available for the determination of milk protein concentration include gel electrophoresis [24], capillary electrophoresis [6, 25], liquid chromatography [26], and immunological techniques [27–29]. However, these methods are less accurate, less reproducible, and sample processing procedures are laborious and time-consuming. Multiple reaction monitoring (MRM) technology has found utility in the quantitation of proteins in complex mixtures [30–32]. Its remarkable sensitivity and selectivity enable the detection and quantification of low abundant substances in complex mixtures. Quantitative protein assays have been developed with targeted MRM methods to analyze protein concentrations in human plasma [33], human serum [34], and bovine milk [35]. However, MRM has not been used to monitor multiple proteins in human milk simultaneously. Our group has recently reported a novel MRM method for quantifying serum IgG and its glycoforms simultaneously [36]. This method yields both protein concentration and site-specific glycosylation quantitation in a single experiment, thereby enabling unprecedented insight into glycosylation.

In this study, we employ the power of MRM, for the first time, to obtain label-free quantitation of the seven most abundant whey proteins: α-lactalbumin, lactoferrin, secretory immunoglobulin A (slGA), immunoglobulin G (IgG), immunoglobulin M (IgM), α1-antitrypsin (A1AT), and lysozyme (LZ). By quantifying unique peptides from each protein, we achieved high reproducibility and low limits of quantitation (LOQ). Furthermore, the site-specific glycosylation of five glycoproteins (LF, sIgA, IgG, IgM, and A1AT) were determined. Quantitation of the glycoforms was performed by normalizing glycopeptides MS response to the protein abundances. This approach removes the contribution of protein concentration to glycan abundances and allows for the simultaneous monitoring of glycosylation across several proteins and several sites. The analytical platform was tested for its reproducibility and LOQ in a 96-well plate format. The study provides the foundation of a general method for the rapid-throughput analysis with quantitation of human milk proteins and their glycoforms. The method can be used to profile the changes in levels of proteins and glycosylation between milk samples.

Experimental procedures

Materials and chemicals

Analytical standards including human milk proteins IgG, LF, α-Lact, IgM, sIgA, and A1AT from human plasma were purchased from Sigma-Aldrich (St. Louis, MO). Human neutrophil lysozyme was purchased from Lee Biosolutions (St. Louis, MO). Human IgA was purchased from Calbiochem (Chicago, IL). Sequencing grade modified trypsin (Cat.# V5111) and dithiothreitol (DTT) were purchased from Promega (Madison, WI). Iodoacetamide (IAA) CAS 74-88-4 was purchased from Sigma-Aldrich (St. Louis, MO).

Human milk samples

Milk samples were collected from three healthy donors enrolled in the UC Davis Lactation Study who gave birth to term infants (>38 weeks). Milk samples were collected on day 28–30 postpartum from one breast and transferred into polypropylene Falcon tubes and frozen immediately in their kitchen freezers (−20 °C) until weekly sample pick up by the study staff. Samples were transported to the lab on dry ice and stored in −80 °C until processing.

Tryptic digestion

Trypsin digestion was first carried out on the seven individual protein standards to profile their peptides and glycopeptides. A 50-μg sample of each protein was dissolved/diluted with 50 mM NH_4HCO_3 prior to reduction and alkylation with 2 μL of 550 mM dithiothreitol (DTT) (60 °C, 50 min) and 4 μL of 450 mM iodoacetamide (IAA) (1 h, in dark) respectively. Then, 1 μg of trypsin in 10 μL of 50 mM NH_4HCO_3 was added, and each protein was digested in a 37 °C water bath for 18 h. The resulting peptide samples were used directly for Q-TOF mass spectrometry (MS) analysis without further sample cleanup.

For rapid throughput quantitation, accurate amounts of protein standards (LF, α-Lact, IgG, and A1AT) were weighed using a micro-balance (Mettler Toledo, XP26) and dissolved in 50 mM NH_4HCO_3 to make 4 mg/mL stock solution. A

50-μL LF stock solution, 50-μL α-Lact, 5-μL A1AT, and 5-μL IgG stock solution were combined to make the standard protein mixture. A 100-μg sample of IgA (62.5 μL conc. 1.6 mg/mL), 20 μg of IgM (18.2 μL conc. 1.1 mg/mL), and 20 μg (18.2 μL conc. 1.1 mg/mL) of LZ solution were then added into the previous solution to make the final standard protein mixture. The standard protein mixture (~209 μL) was transferred to a single well in a 96-well plate. For tryptic digestion, 175 μL of 50 mM NH_4HCO_3 was added to 25 μL of whole milk in the same 96-well plate with the standard protein mixture. The milk samples and standard mixtures were reduced with 2 and 4 μL of 550 mM dithiothreitol (DTT) followed by incubation for 50 min at 60 °C. A 4 and 8-μL 450 mM iodoacetamide (IAA) was then added to the milk samples and the standard mix, respectively, followed by carboxymethylation by incubation for 60 min at room temperature in the dark. Two micrograms of trypsin in 20 μL of 50 mM NH_4HCO_3 was added to the samples, prior to the digestion for 18 h at 37 °C in an incubator (Fisher Scientific, Pittsburgh, PA).

The digests were purified on C18 96-well cartridge plate (Glygen, Columbia, MD). The C18 plate was preconditioned successively with two volumes (200 μL for each volume) of pure water in 0.1 % TFA, two volumes of 100 % acetonitrile (ACN), and three volume of pure water in 0.1 % TFA, by adding each solvent and centrifuging the plate in Eppendorf 5810R centrifuge (Eppendorf, Hauppauge, NY) at 1700 rpm in room temperature. The tryptic digests were loaded on the plate and then washed with three volumes of pure water in 0.1 % TFA by centrifugation, prior to eluting with two volumes of 40 % ACN in 0.1 % TFA and one column of 80 % ACN in 0.1 % TFA and dried to completion.

Instrumentation

A nano-HPLC-Chip Q-TOF instrument using the Agilent 1200 series microwell-plate autosampler (maintained at 6 °C by the thermostat), capillary pump, nano pump, HPLC-Chip interface, and the Agilent 6520 Q-TOF MS (Agilent Technologies, Inc., Santa Clara, CA) were used in this study.

For the peptides and glycopeptides, a reverse-phase nano-HPLC Chip (G4240-62001, Agilent Technologies, Inc., Santa Clara, CA) with a 40-nL enrichment column and 43 × 0.075 mm ID analytical column was used. The column was packed with ZORBAX C18 (5 μm pore size) stationary phase. The mobile phase for tryptic peptides consisted of 0.1 % formic acid in 3 % ACN in water (*v*/*v*) as solvent A and 0.1 % formic acid in 90 % ACN in water (*v*/*v*) as solvent B. The nano pump gradient was performed on the analytical column to separate the tryptic peptides with a flowrate at 0.4 μL /min. The peptides were eluted in 60 min with the following gradient: 3 % B (0.00–2.50 min), 3 to 16 % B (2.50–20.00 min), 16 to 44 % B (20.00–30.00 min), 44 to 100 % B (30.00–35.00 min), and 100 % B (35.00–45.00 min) and re-equilibrated at 3 % B from 45.01 to 60 min.

The Agilent 6520 Q-TOF MS was operated in the positive ion mode for MS and MS/MS of the tryptic peptides. The recorded mass ranges were *m*/*z* 500–3000 for MS only and *m*/*z* 50–3000 for MS/MS. Acquisition rates were 7.99 spectra/s for MS scan and 3 spectra/s for MS/MS scan. The drying gas temperature was set at 325 °C with a flow rate of 4 L/min. All mass spectra were internally calibrated using the G1969-85000 ESI tuning mix (Agilent Technologies, Inc., Santa Clara, CA), with reference masses at *m*/*z* 922.010, and 1521.971 in the positive ion mode. In MS/MS mode, the collision energies for the tryptic peptides were calculated as follows:

$$V_{\text{collision}}(eV) = 3.6\left(\frac{m/z}{100\text{Da}}\right) - 4.8$$

The peptide samples were analyzed and quantified using an Agilent 1290 infinity LC system coupled to an Agilent 6490 triple quadrupole mass spectrometer (Agilent Technologies, Santa Clara, CA) using a 96-well injection plate (Eppendorf, Hauppauge, NY). An Agilent Eclipse plus C18 (RRHD 1.8 μm, 2.1 x 100 mm) was used for UPLC separation.

The standard protein mix was diluted serially in nano pure water to obtain a calibration curve for protein quantitation. The human milk samples were reconstituted with 100 μL nano pure water. A 1.0-μL sample was injected for each run. Three replicate injections were performed for each protein standard mix to evaluate the instrument repeatability. One nano pure water blank was run after every four sample runs to observe potential carry overs.

The mobile phase for tryptic peptides consisted of 0.1 % formic acid in 3 % ACN in water (*v*/*v*) as solvent A and 0.1 % formic acid in 90 % ACN in water (*v*/*v*) as solvent B. The 16-min gradient was as follows: 0 min at 2.0 % B, 1.5 min at 15.0 % B, 3 min at 25 % B, 4 min at 30 % B until 7 min, 10 min at 35 % B, 11 min at 40 % B, and 12 min at 100 % B; the column was washed at 100 % B from 12.1 to 14 min and re-equilibrated at 2.0 % B from 14.1 to 16 min.

The MS was operated in the positive mode. Q1 and Q3 were operated at unit resolution. The optimal parameters used were as follows: drying gas (N_2) temperature and sheath gas (N_2) temperature 290 °C, drying gas flow rate 11 L/min, sheath gas flow rate 12 L/min, nebulizer pressure 30 psi, capillary voltage 1800 V, and fragmentor voltage 280 V. RF voltage amplitude of high pressure and low pressure ion funnel were 100 and 60 V, respectively.

The dynamic MRM mode was used, whereby the transitions were monitored only when the target analyte was eluted. The cycle time was fixed at 500 ms, while the dwell time depended on the number of concurrent transitions monitored.

The MRM results were analyzed using Agilent MassHunter Quantitative Analysis B.6.0 software. The peak areas were integrated by the software and used for quantitation. The limit of detection (LOD) and limit of quantitation (LOQ) were defined as S/N ≥3 and 10, respectively.

Data processing

Tryptic peptide MS/MS data from Q-TOF MS were analyzed using X! Tandem (www.thegpm.org). X! Tandem was set to search the Swissprot human proteome database. X! Tandem was searched with a fragment ion mass tolerance of 80 ppm and a parent ion tolerance of 100 ppm with one trypsin missed cleavages allowed. Iodoacetamide derivative of cysteine was specified in X! Tandem as a fixed modification. Deamination of asparagine and glutamine, oxidation of methionine, and tryptophan were specified in X! Tandem as variable modifications. Peptides for each protein in the standard protein mix were selected based on the peptide profile. Glycopeptide identification from glycoproteins (LF, sIgA, IgG, IgM, and antitrypsin) was performed using in-house software, GPFinder. Carbohydrate oxonium ions, such as, *m*/*z* 204.08 (HexNAc), *m*/*z* 366.14 (Hex1HexNAc1), *m*/*z* 292.09 (Neu5Ac), and *m*/*z* 657.24 (Hex1HexNAc1Neu5Ac1) were used as diagnostic fragments for glycopeptides. The glycopeptide compositions were assigned on the basis of their exact mass and the fragmentation pattern.

Results and discussion

Peptide and glycopeptide profiling

Standard LF, α-Lact, sIgA, IgG, IgM, A1AT, and LZ were digested using trypsin prior to the analysis with LC-Q-TOF MS/MS to evaluate the fragmentation behavior of the respective peptides and glycopeptides. During the protein digestion, DTT was used to reduce the cysteine disulfide bonds. The free –SH groups were subsequently alkylated using IAA to prevent them from reforming. All the observed cysteine residues were Carbamidomethylated. Our group has reported the peptide selection for quantitation of serum IgG [36]. fA similar strategy was applied for the other six proteins in milk. However, the predominant immunoglobulin in breast milk, sIgA, is a protein complex consisting of two identical IgA monomers (IgA1 or IgA2), joined together via a 16-kDa joint chain (J chain), and a secretory component (SC). It is not possible to find a common peptide for all the four polypeptides; therefore, quantitation was not possible for sIgA. Instead, IgA standard was used to obtain IgA concentration in human milk. The tryptic peptides YLTWASR and VAAEDWK, which are common to both IgA1 and IgA2, were selected for quantitation of IgA. In Fig. S1a (see Electronic Supplementary Material, ESM), the MSMS spectrum of the tryptic peptide YLTWASR is shown, thereby illustrating the abundances of b- and y-ions. Abundant b- and/or y-ions were selected for the MRM analysis. Peptides TPLTATLSK for IgA1, DASGATFTWTPSSGK for IgA2, GSVTFHCALGPEVANVAK for SC, and IIVPLNNR for the J chain were used for glycosylation quantitation. The tandem mass spectra of the SC and J chain peptides are shown in Fig. S1b and S1c (see ESM).

Compositions of glycopeptides obtained from trypsin digestion were assigned based on the MS/MS data and the accurate precursor ion mass measurement. Previous studies from our group on the analysis of tryptic glycopeptides with collision-induced dissociation (CID) experiments revealed detailed and comprehensive glycan compositional information for IgG subclasses [36]. Glycosidic bond cleavages (B- and Y-type ions) were the major products including *m*/*z* 292.09 (Neu5Ac), 274.08 (Neu5Ac–H_2O), 204.08 (HexNAc), 366.14 (Hex+HexNAc), and 657.24 (Hex+HexNAc+Neu5Ac). Tandem spectra of glycopeptides from two N-glycosites of LF with the same glycan composition are depicted in Fig. 1a, b. Due to the labile nature of sialic acid residues and their positions at the terminus, the initial loss of sialic acid was commonly observed with the sialylated glycopeptides. Following the sequential neutral losses of Neu5Ac, Hex and HexNAc loss leads to the glycopeptide fragment (peptide+HexNAc). The presence of the peptide+HexNAc is valuable for validating the assignment of parent glycopeptide [37, 38]. Glycopeptides from each glycoprotein were examined in the similar manner, thereby revealing the site-specific glycosyation with trypsin digestion.

Figure 2 shows the site heterogeneity of the five glycoproteins (LF, IgG, IgM, A1AT, and sIgA). LF is an abundant milk glycoprotein with three potential glycosylation sites, of which two sites are highly occupied (^{156}N and ^{497}N) while a third site (^{642}N) is rarely occupied [39, 40]. LF has long been imbued with the role of bacterial defense by acting as decoys and occupying binding sites on bacteria, thereby prohibiting them from binding to host cells [39–42]. Less known are the roles of glycosylation in this function. Previous binding studies of bacteria to host epithelial cells in our lab show that LF blocks the binding of pathogens to host cells [7]. For example, cleaving all the N-glycans diminishes its ability to block *Escherichia coli*. Removing fucose increases the ability of *Salmonella typhimurium* to bind to epithelial cells while removing sialic acid increases the ability of *Salmonella enteritidis* to adhere to host cells. The efficacy of LF is mediated by specific glycan structures. However, the site-specific glycosylation of LF was still not fully elucidated. Here in Fig. 2a, glycan site heterogeneity of LF is shown. The two major N-glycosites were characterized with mainly sialylated glycans, which most times may act as receptors for many viruses and pathogenic bacteria, enabling the viruses to gain

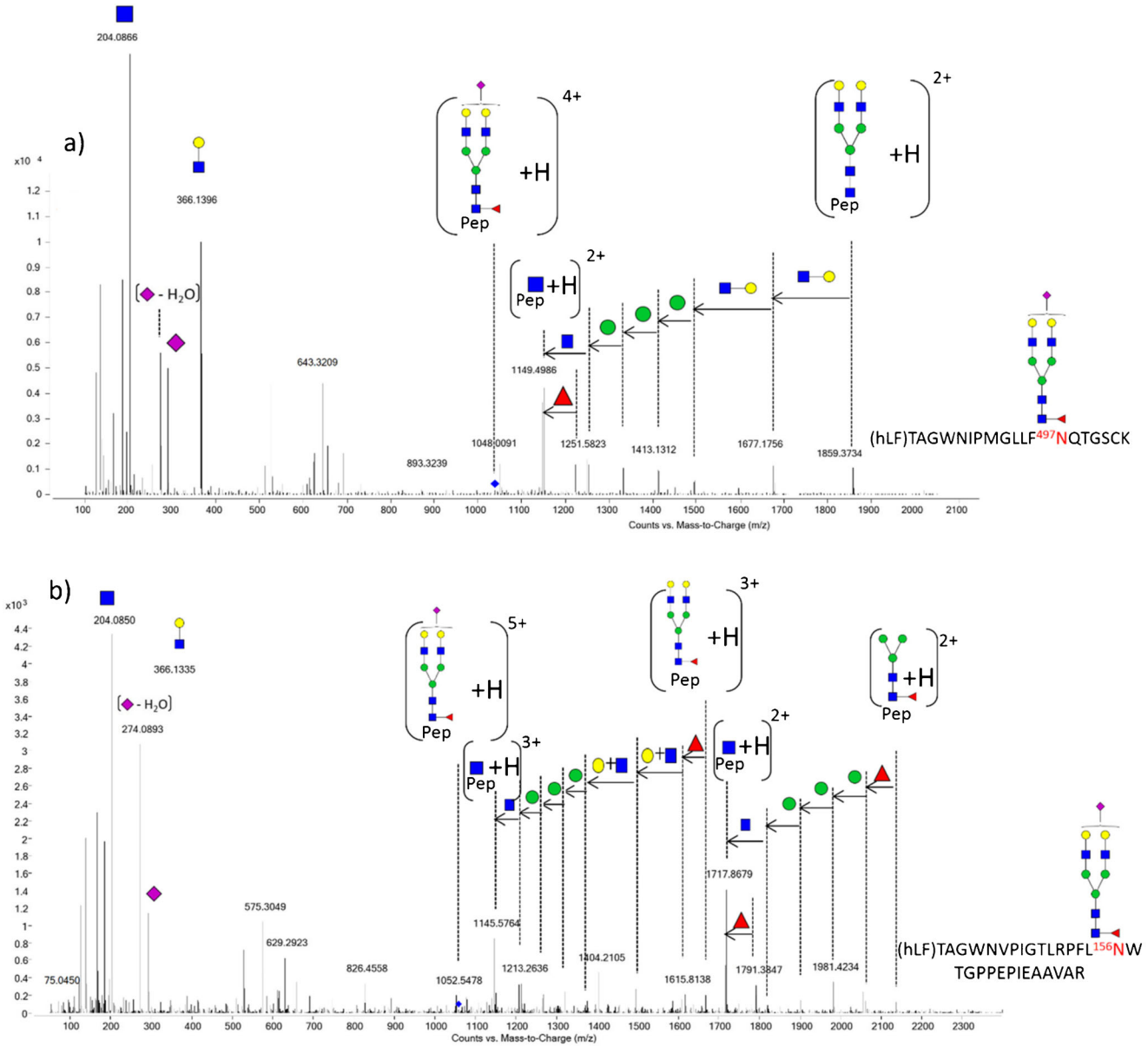

Fig. 1 Representative Q-TOF tandem mass spectra of glycopeptides. **a** MS/MS spectrum of glycopeptide $Hex_5HexNAc_4Fuc_1Neu5Ac_1$-TAGWNIPMGLLF^{497}NQTGSCK from LF. **b** MS/MS spectrum of $Hex_5HexNAc_4Fuc_1Neu5Ac_1$- TAGWNVPIGTLRPFL^{156}NWTGPPEPIEAAVAR from LF. *Green circles*, *yellow circles*, *blue squares*, *red triangles*, and *purple diamonds* represent mannose, galactose, GlcNAc, fucose, and NeuAc residues, respectively

entry into human cells [43–47]. As shown in Fig. 2b, glycopeptides from four subclasses of IgG were profiled, and the resulting glycan heterogeneity corresponded well with what has been previously reported [36, 48, 49].

In the heavy chain of IgM, three N-glycosites (^{46}N, ^{209}N, and ^{272}N) were reported to be occupied with complex type N-glycans, while the other two (^{279}N and ^{439}N) were occupied with high mannose type [50–52]. Detailed site-specific glycosylation mapping has not yet been reported. Due to the limitations often inherent with trypsin digestion, glycosites ^{272}N and ^{279}N were close together and yielded one tryptic peptide so the site-specific information for the individual site was not available. However, as shown in Fig. 2c, the other sites were readily characterized. ^{439}N was occupied with high mannose glycans ranging in size from $Man_5GlcNAc_2$ to $Man_9GlcNAc_2$, while ^{46}N and ^{209}N were occupied by complex glycans with various degrees of sialylation.

A1AT is an important human glycoprotein that belongs to the family of serpins and is the major inhibitor of neutrophil elastase [53, 54]. It has been shown that glycosylation increases the stability of A1AT [55, 56]. A1AT was characterized with three N-glycosites that were mainly occupied with complex type N-glycans (Fig. 2d). The results of our study also matches well with literature, [57–59] where complex N-

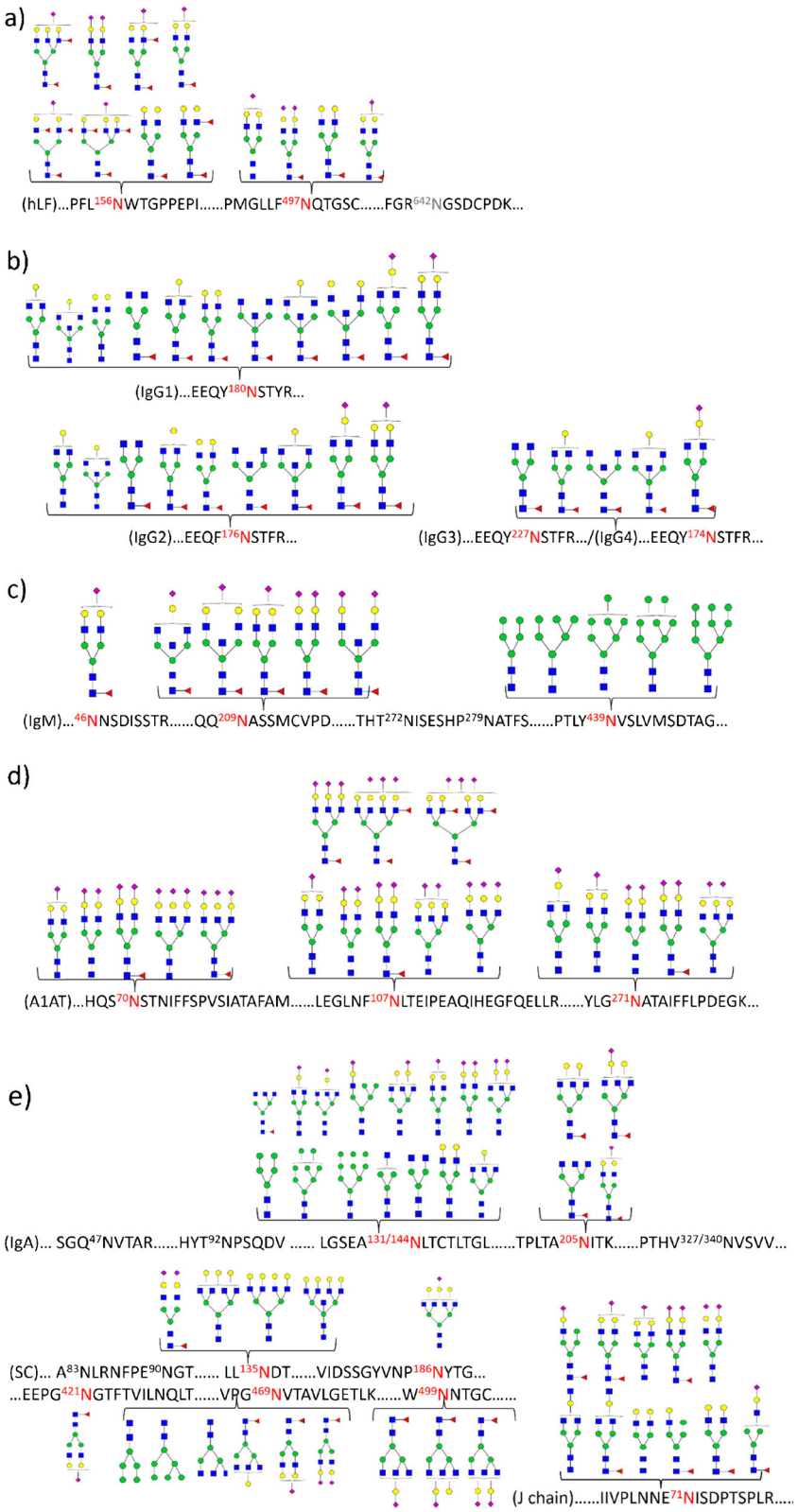

Fig. 2 Glycan site-heterogeneity of human milk glycoproteins: **a** LF, **b** IgG, **c** IgM, **d** A1AT, and **e** sIgA. *Green circles*, *yellow circles*, *blue squares*, *red triangles*, and *purple diamonds* represent mannose, galactose, GlcNAc, fucose, and NeuAc residues, respectively

glycans, mostly di- and triantennary with sialic acids, were reported for all three sites. However, peaks for ^{70}N were not observed in the MRM profiling probably due to the low occupancy of this glycosite. Therefore, in this study, only two sites from A1AT were monitored and quantified in the MRM assays.

The protein sIgA is a major antibody found in external secretions such as human milk, and it plays a major role in

the protection of mucosal surfaces [60, 61]. In Fig. 2e, the site-specific glycosylation was determined using trypsin digestion for each component of sIgA including the secretory component, IgA1, IgA2, and the J chain. Due to either the resistance of many glycoproteins to undergo tryptic digestion or the relatively large size of glycopeptides, glycans at several sites were not observed. The results obtained with the trypsin, while incomplete matched well with those using non-specific proteases. Furthermore, the goal of this study was to quantify the proteins and their glycoforms; therefore, the more specific protease trypsin was selected and characterized to yield reproducible glycopeptides.

Configuration and Optimization of MRM Assay

The main concern with using QqQ mass spectrometers for targeted analysis is the low mass selection resolution that may cause interference by other ions particularly in a complicated matrix such as milk [32]. To reduce the chances of potential interferences, two peptides for each protein were selected to increase specificity and selectivity of the quantitative assay in human milk. The selection for peptides followed several rules that have been discussed in a recent study from our laboratory [36]. Firstly, the selected peptides should be unique to the protein and unmodified by other PTMs, such as deamination and oxidation. Secondly, two peptides from each protein are chosen for quantitation in MRM. The exception of the second rule was LZ where the short length yielded only one peptide with no potential PTMs.

MRM transitions were optimized for these peptides for their quantifier, qualifier, retention time, and collision energy. For IgG and sIgA, the peptides common to all four IgG subtypes and to both IgA1/IgA2 were selected for overall quantitation. For example, the quasimolecular ion ($[M + 2H]^{2+}$ m/z 409.7) for the IgA1/2 peptide VAAEDWK was selected as the precursor ion, while m/z 648.3 was selected as the fragment ion. Additionally, a second transition from the same precursor ion to fragment ion m/z 719.4 was used as qualifier. It is unlikely that an interference may share both quantifier and qualifier, giving the method high specificity and selectivity with the targeted peptides. A dynamic MRM method was applied to specifically monitor one analyte at a time, which reduced the number of concurrent transitions. The retention time for the above peptide was determined to be 2 min, and the optimized fragmentation voltage was 9 eV. Every MRM transition was optimized with a specific retention time to reduce the duty cycle. Summarized in Table 1a are the transitions for all peptides monitored with their precursor mass, product mass, retention time, and fragmentation voltage.

Reproducibility of the selected peptides was determined by relative standard deviation (RSD) of the peak areas based on triplicates performed on different days (Table 1a). The RSD were generally below 10 % illustrating the high repeatability of the method.

As shown in Fig. 1, oxonium ions corresponding to small glycan fragments m/z 204.08 (HexNAc) and m/z 366.14 (Hex+HexNAc) were abundant and therefore chosen as the product ion for most of the glycopeptide MRM transitions. However, for some of the high mannose-containing glycopeptides, the fragment peptide+HexNAc was found to yield better responses. For example, for the site ^{439}N of IgM, which contains primarily high-mannose type N-glycans, the product ion selected correponded to m/z 1284.7 (STGKPTLY^{439}NVSLVMSDTAGTCY+HexNAc). Listed in Table 1b are the glycopeptides from the five glycoproteins discussed above including more than 100 glycopeptides. It should be noted that the retention times of the glycopeptides on C18 stationary phases rely mainly on the peptide moiety of the glycoconjugates. Therefore, glycopeptides that originate from the same site and thus share the same peptide generally elute closely together. Due to the limitations in duty cycles, one transition was selected for each glycopeptide monitored. Dynamic MRM help reduced the effects of co-elution of the glycopeptides and increased the sensitivity of the analysis.

An example chromatogram obtained from the MRM transitions of the standard protein mixture is shown in Fig. 3. Good separation was obtained within the 16 min UPLC gradient. Most of the glycopeptides eluted after 4 min while the nonglycosylated peptides eluted between 2 and 4 min (Fig. 3a). This difference fortunately reduced the charge competition during electrospray ionization resulting in higher glycopeptide sensitivity because peptides ionize more readily than glycopeptides.[62–64] Due to the ionization differences, the peptides MS signal (shown in black in Fig. 3a) are significantly higher than the glycopeptides MS signal. Good separation between the peptides and glycopeptides is critical for MRM of glycopeptides. Peptide peaks from the seven proteins and glycopeptide peaks from the five glycoproteins are shown in Fig. 3b, c, respectively. This method provides a general and sensitive analysis that can be used for a large number of proteins and their glycoforms.

Quantitation of Human Milk Proteins

The relative abundances of the seven proteins in milk varies considerably from ~20 % for α-Lact and LF, ~10 % for sIgA, ~5 % for LZ, and <1.0 % for IgG, IgM, and A1AT [65, 66]. Different concentrations of each standard protein were prepared to produce a standard mixture (as 1× stock solution) consisting of 4.0 mg/mL for α-Lact and LF, 2.0 mg/mL for IgA, 0.4 mg/mL for LZ, IgG, IgM, and A1AT. In order to quantitate the targeted proteins, a series dilution of the standard protein mix was used to build the calibration curve from 5000×, 2000×, 1000×, 500×, 100×, 50×, 20×, 10×, 5×, 2×, and 1× (ESM Table S1). A 1.0-μL volume of each dilution was analyzed. The resulting calibration curves using one

Table 1 MRM transitions used to monitor a) peptides. Relative standard deviations (RSDs) are based on triplicates performed on different days. The limit of quantitation was determined with S/N >10. MRM transitions used to monitor a) peptides b) glycopeptides

a)

Protein	Peptide	Precursor ion (*m*/*z*)	Product ion (*m*/*z*)	RT (min)	Delta RT (min)	Collision energy (eV)	RSD %	LOQ (fmol)
A-Lact	GIDYWLAHK	551.8	932.5	3.1	0.5	18	6.6	50
		551.8	654.4	3.1	0.5	18		
A-Lact	FLDDDITDDIMCAK	836.4	953.4	4.1	0.5	27	11.1	50
		836.4	1066.5	4.1	0.5	27		
LF	LRPVAAEVYGTER	487.6	625.3	2.34	0.5	10	2.6	20
		487.6	737.4	2.34	0.5	10		
LF	DGAGDVAFIR	510.8	506.3	3.03	0.5	13	2.0	10
		510.8	605.4	3.03	0.5	13		
IGA	YLTWASR	448.7	620.3	2.87	0.5	12	2.3	10
		448.7	519.3	2.87	0.5	12		
IGA	VAAEDWK	409.7	648.3	2	0.5	8	6.0	25
		409.7	719.4	2	0.5	8		
IGG	DTLMISR	418.2	506.3	2.52	0.5	9	0.6	2
		418.2	619.4	2.52	0.5	9		
IGG	NQVSLTCLVK	581.3	243.1	3.25	0.5	14	8	20
		581.3	342.2	3.25	0.5	14		
IGM	YAATSQVLLPSK	639.4	331.2	2.8	0.5	15	5.4	2
		639.4	947.6	2.8	0.5	15		
IGM	FTCTVTHTDLPSPLK	572.95	734.9	3	0.5	9	2.4	2
		572.95	654.9	3	0.5	9		
A1AT	LSITGTYDLK	555.8	910.5	3.15	0.5	18	4.7	10
		555.8	797.4	3.15	0.5	18		
A1AT	SVLGQLGITK	508.3	829.5	3.46	0.5	14	3.0	10
		508.3	716.4	3.46	0.5	14		
LZ	STDYGIFQINSR	700.8	764.4	3.57	0.5	20	6.5	50
		700.8	489.3	3.57	0.5	20		
SC	GSVTFHCALGPEVANVAK	619.7	414.2	3	0.5	14	5.2	-
		619.7	442.7	3	0.5	14		
IGA1	TPLTATLSK	466.3	620.4	2.5	0.5	15	0.8	-
		466.3	415.8	2.5	0.5	15		
IGA2	DASGATFTWTPSSGK	756.9	475.3	3.08	0.5	22	5.1	-
		756.9	863.4	3.08	0.5	22		
J	IIVPLNNR	469.8	613.3	2.84	0.5	12	1.4	-
		469.8	712.4	2.84	0.5	12		
IGG1	GPSVFPLAPSSK	593.83	846.5	3.43	0.5	20	5.9	-
		593.83	699.4	3.43	0.5	20		
IGG2	TTPPMLDSDGSFFLYSK	636	852.4	4.5	0.5	13	8.1	-
		636	843.4	4.5	0.5	13		
IGG3	WYVDGVEVHNAK	472.91	534.3	2.7	0.5	6	6.1	-
		472.91	697.4	2.7	0.5	6		
IGG4	TTPPVLDSDGSFFLYSR	634.98	1217.6	4.48	0.5	9	7.5	-
		634.98	425.2	4.48	0.5	9		

b)

Protein	Glycopeptide	Precursor ion (*m*/*z*)	Product ion (*m*/*z*)	RT (min)	Delta RT (min)	Collision energy (eV)
IGG	IGG H4N4F1_1	932.8	204.1	1.38	0.5	15
IGG	IGG H5N4_1	938.1	366.1	1.38	0.5	14
IGG	IGG H5N4F1_1	986.8	366.1	1.38	0.5	15

Table 1 (continued)

IGG	IGG H3N4F1_1	878.8	204.1	1.4	0.5	13
IGG	IGG H4N4_1	884.1	204.1	1.4	0.5	14
IGG	IGG H4N4F1_3_4	927.4	204.1	1.4	0.5	14
IGG	IGG H4N5F1_3_4	995.1	204.1	1.4	0.5	15
IGG	IGG H4N5F1_1	1000.5	204.1	1.4	0.5	16
IGG	IGG H5N5F1_1	1054.5	366.1	1.4	0.5	17
IGG	IGG H3N5F1_3_4	941.1	204.1	1.41	0.5	15
IGG	IGG H3N5F1_1	946.5	204.1	1.42	0.5	15
IGG	IGG H4N4F1S1_3_4	1024.5	204.1	1.45	0.5	25
IGG	IGG H5N4F1S1_3_4	1078.4	366.1	1.45	0.5	17
IGG	IGG H5N4F1S1_1	1083.8	366.1	1.45	0.5	17
IGG	IGG H4N4F1S1_1	1029.8	204.1	1.47	0.5	16
IGG	IGG H4N5_1	951.7	204.1	1.7	0.5	15
IGG	IGG H4N4_2	873.4	204.1	2.1	0.5	13
IGG	IGG H4N4F1_2	922.1	204.1	2.1	0.5	25
IGG	IGG H3N5F1_2	935.8	204.1	2.1	0.8	14
IGG	IGG H4H5_2	941.1	204.1	2.1	0.5	15
IGG	IGG H5N4F1_2	976.1	366.1	2.1	0.5	15
IGG	IGG H4N4F1S1_2	1019.1	204.1	2.1	0.5	25
IGG	IGG H4N5F1_2	989.9	204.1	2.12	0.5	15
IGG	IGG H5N4F1S1_2	1073.1	366.1	2.2	0.5	25
IGM	IGM-209 H5N4F1S1	1100.5	366.1	3.1	0.5	19
IGM	IGM-46 H5N4F1S1	1115.5	366.1	3.1	0.5	25
IGM	IGM-209 H5N5F1S1	1151.3	366.1	3.1	0.5	25
J	J H5N3F1	1238.6	204.1	3.1	0.8	33
J	J H5N4	1257.6	366.1	3.1	0.8	30
J	J H4N5	1271.3	366.1	3.1	0.8	33
IGM	IGM-209 H4N5F1S1	1110.8	366.1	3.12	0.5	24
J	J H4N5F1	990.2	204.1	3.13	0.5	25
IGM	IGM-209 H5N4F1S2	1173.3	366.1	3.15	0.5	23
IGM	IGM-209 H5N5F1S2	1224.1	366.1	3.16	0.5	25
J	J H5N4F1S1	1052.8	366.1	3.2	0.5	24
J	J H5N3F1S1	1002	366.1	3.24	0.5	28
J	J H5N4S1	1016.2	204.1	3.25	0.5	25
J	J H5N4F1S2	1125.5	366.1	3.33	0.5	30
IGM	IGM-439 H6N2	1248.5	1284.7	3.66	0.5	24
IGM	IGM-439 H9N2	1058.3	1284.7	3.68	0.5	27
IGM	IGM-439 H8N2	1356.6	1284.7	3.68	0.5	27
IGM	IGM-439 H5N2	1194.5	1284.7	3.7	0.5	27
IGM	IGM-439 H7N2	1302.6	1284.7	3.7	0.5	27
SC	SC-499 H4N5F1S1	1019.7	204.1	4.15	0.5	25
SC	SC-499 H5N5F1S1	1060.2	366.1	4.25	0.8	25
SC	SC-499 H5N5F1S2	1132.9	366.1	4.32	0.8	26
LF	LF-497 H5N4F1	966.7	204.1	4.65	0.8	28
A1AT	AT-271 H5N4S2	990.9	204.1	4.65	0.8	29
A1AT	AT-271 H5N4F1S2	1027.4	204.1	4.65	0.5	25
A1AT	AT-271 H5N4S1	1223.9	366.1	4.68	0.5	29
A1AT	AT-271 H6N5S3	1154.98	204.1	4.7	0.5	30
A1AT	AT-271 H4N3S1	1102.2	204.1	4.85	0.5	40
LF	LF-497 H5N4F1S1	1039.4	204.1	4.86	0.8	33
LF	LF-497 H5N4S1	1002.9	204.1	4.96	0.8	32
LF	LF-497 H5N4F1S2	1112.2	204.1	5.05	0.8	35
IGA	IGA-131/144 H9N2	966.5	204.1	5.3	0.8	30
SC	SC-469 H5N2	872.1	204.1	5.4	0.5	20
SC	SC-135 H6N6	1092.5	204.1	5.4	0.5	28
IGA	IGA2-131 H6N2	1168	204.1	5.4	0.8	36
SC	SC-469 H3N5	967.1	204.1	5.5	1	25
IGA	IGA2-205 H3N5F1	869.4	204.1	5.55	0.5	23
SC	SC-469 H6N2	926.1	366.1	5.55	1	20
IGA	IGA-131/144 H8N2	934.1	204.1	5.6	1	29
SC	SC-469 H5N4F1S2	937.9	204.1	5.6	1	24
IGA	IGA-131/144 H5N4	1147.3	204.1	5.6	1	37
IGA	IGA-131/144 H4N5	1157.6	204.1	5.6	1	31
IGA	IGA1-144 H5N5	1198.1	366.1	5.6	0.8	25

Table 1 (continued)

SC	SC-135 H5N4F1S2	906.2	204.1	5.65	0.5	30
IGA	IGA-131/144 H3N4	1066.3	204.1	5.65	0.5	34
IGA	IGA-131/144 H5N2	1045.8	204.1	5.7	0.8	33
IGA	IGA1-144 H3N5	1117.1	366.1	5.7	0.8	25
SC	SC-135 H7N7	1173.5	204.1	5.7	0.5	30
SC	SC-135 H6N7	1143.3	204.1	5.73	0.8	30
IGA	IGA-131/144 H3N3	1015.5	204.1	5.75	0.8	32
SC	SC-135 H7N6	1133	366.1	5.75	0.8	28
IGA	IGA-131/144 H3N5F1	1102.8	204.1	5.8	0.5	32
IGA	IGA1-144 H5N4S2	1292.9	366.1	5.8	0.5	30
IGA	IGA-131/144 H5N4S2	1034.5	204.1	5.9	0.5	32
LF	LF-156 H5N4F1	1250.6	204.1	5.9	0.8	35
SC	SC-186 H6N6S1	1252.6	366.1	5.9	0.8	32
LF	LF-156 H5N4F2	1287.1	204.1	5.9	0.8	44
IGA	IGA-131/144 H5F4S1	976.3	204.1	6	1	24
IGA	IGA2-205 H5N5F1	977.5	366.1	6	0.8	25
IGA	IGA-131/144 H5N5S1	1016.9	366.1	6.05	0.8	25
IGA	IGA-131/144 H4N5S1	984.5	204.1	6.15	0.8	31
LF	LF-156 H6N5F3S1	1190.3	366.2	6.4	0.8	26
LF	LF-156 H6N5F2S1	1161.1	204.1	6.5	0.8	36
IGA	IGA-131/144 H5N3S1	1169.3	204.1	6.5	0.8	43
IGA	IGA2-205 H5N4F1S1	1006.8	366.1	6.7	0.8	25
IGA	IGA-131/144 H4N4S1	1179.6	204.1	6.7	0.8	41
LF	LF-156 H5N4F2S1	1088.1	204.1	6.88	0.8	33
SC	SC-469 H4N5F1	1069.8	366.1	6.95	0.8	28
LF	LF-156 H5N4F1S1	1058.9	204.1	7	0.8	35
IGA	IGA2-205 H5N5F1S1	1074.5	366.1	7	0.8	25
IGA	IGA-131/144 H5N5S2	1075.1	366.1	7	0.8	25
SC	SC-469 H5N4F1S1	1153.2	366.1	7	0.8	30
SC	SC-421 H5N4F1S1	1116.3	366.1	7.15	0.8	30
LF	LF-156 H5N4F3S1	1117.3	204.1	7.15	0.8	36
LF	LF-156 H5N4F1S2	1117.1	204.1	8.4	0.8	35
A1AT	AT-271 H5N4S2 Missed cleavage site	958.44	204.1	9.25	0.8	25
A1AT	AT-107 H5N4S2	1180.12	204.1	9.87	0.5	36
A1AT	AT-107 H5N4F1S2	1209.33	204.1	9.97	0.5	36
A1AT	AT-107 H7N6F2S3	1202.51	204.1	10	0.5	36
A1AT	AT-107 H6N5S3	1311.34	204.1	10.35	0.5	45
A1AT	AT-107 H6N5F1S3	1340.59	204.1	10.35	0.5	45

Dynamic MRM was used. Delta retention time is the retention time window for the target transition

H hexose, *N* HexNAc, *F* fucose, *S*, *N*-acetyl neuraminic acid

peptide from each protein is shown in Fig. 4. The calibration curve was linear over at least two orders of magnitude for the concentration range. The calibration curves were fitted linearly with R^2 from 0.99 to 0.999. Limit of quantitation (LOQ) was defined by the S/N>10. The LOQ of all seven targeted proteins are listed in Table 1.

The concentration of each protein in milk was determined by fitting its unique peptide to the linear regression curve. With two peptides selected for each protein (except for LZ), the average was used yielding variations of less than 20 % (data not shown). Tryptic digestion is affected by the local activity of the enzyme. It is widely known that different amino acid modifications may generate different efficiencies of the trypsin digestion and may yield missed cleavages. Hence, the average of different peptides from the same protein is a reliable way of diminishing the potential variations in enzymic activity.

The overall goal of this study is to develop a rapid-throughput method to quantify human milk protein concentrations and their glycosylation levels in different samples. To this end, mature human milk samples (>25 days of lactation) from three healthy donors were analyzed in triplicates (nine milk samples in total) along with the standard mixtures by randomizing the sample pool in a 96-well plate and trypsin digested as discussed in the experimental section above. An example of chromatograms obtained from the MRM

Fig. 3 Total MRM chromatogram for seven standard protein mix using ▶ UPLC-C18 chromatography. MRM chromatograms for **a** peptides and glycopeptides, **b** peptide with assigned transitions, and **c** glycopeptides with assigned transitions. The MRM transitions are shown in Table 1. One MRM transition was monitored for each glycopeptide; two MRM transitions were monitored for each peptide

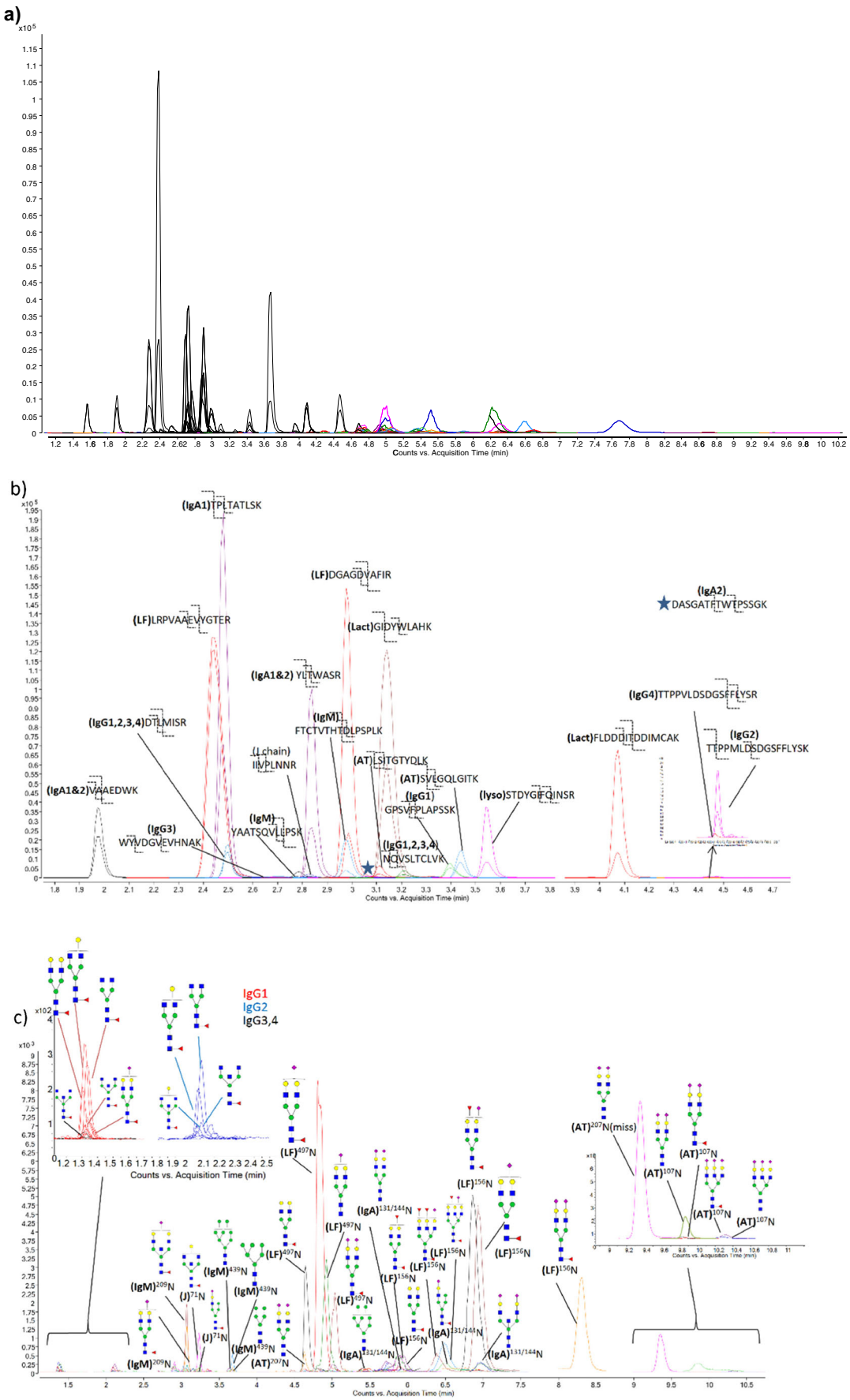
a)
Counts vs. Acquisition Time (min)
b)
(IgA1)TPLTATLSK
(LF)DGAGDVAFIR
(LF)LRPVAAEVYGTER
(Lact)GIDYWLAHK
(IgA2)
DASGATFTWTPSSGK
(IgA1&2) YLTWASR
(IgG4)TTPPVLDSDGSFFLYSR
(IgG1,2,3,4)DTLMISR
(IgM)
FTCTVTHTDLPSPLK
(Lact)FLDDDITDDIMCAK
(IgG2)
TTPPMLDSDGSFFLYSK
(L chain)
IIVPLNNR
(AT)LSITGTYDLK
(IgA1&2)VAAEDWK
(AT)SVEGQLGITK
(IgG1)
GPSVFPLAPSSK
(lyso)STDYGIFQINSR
(IgG3)
WYVDGVEVHNAK
(IgM)
YAATSQVLLPSK
(IgG1,2,3,4)
NQVSLTCLVK
Counts vs. Acquisition Time (min)
c)
IgG1
IgG2
IgG3,4
Counts vs. Acquisition Time (min)
(LF)497N
(IgA)131/144N
(LF)156N
(IgM)209N
(J)71N
(IgM)439N
(AT)207N
(AT)207N(miss)
(AT)107N
Counts vs. Acquisition Time (min)

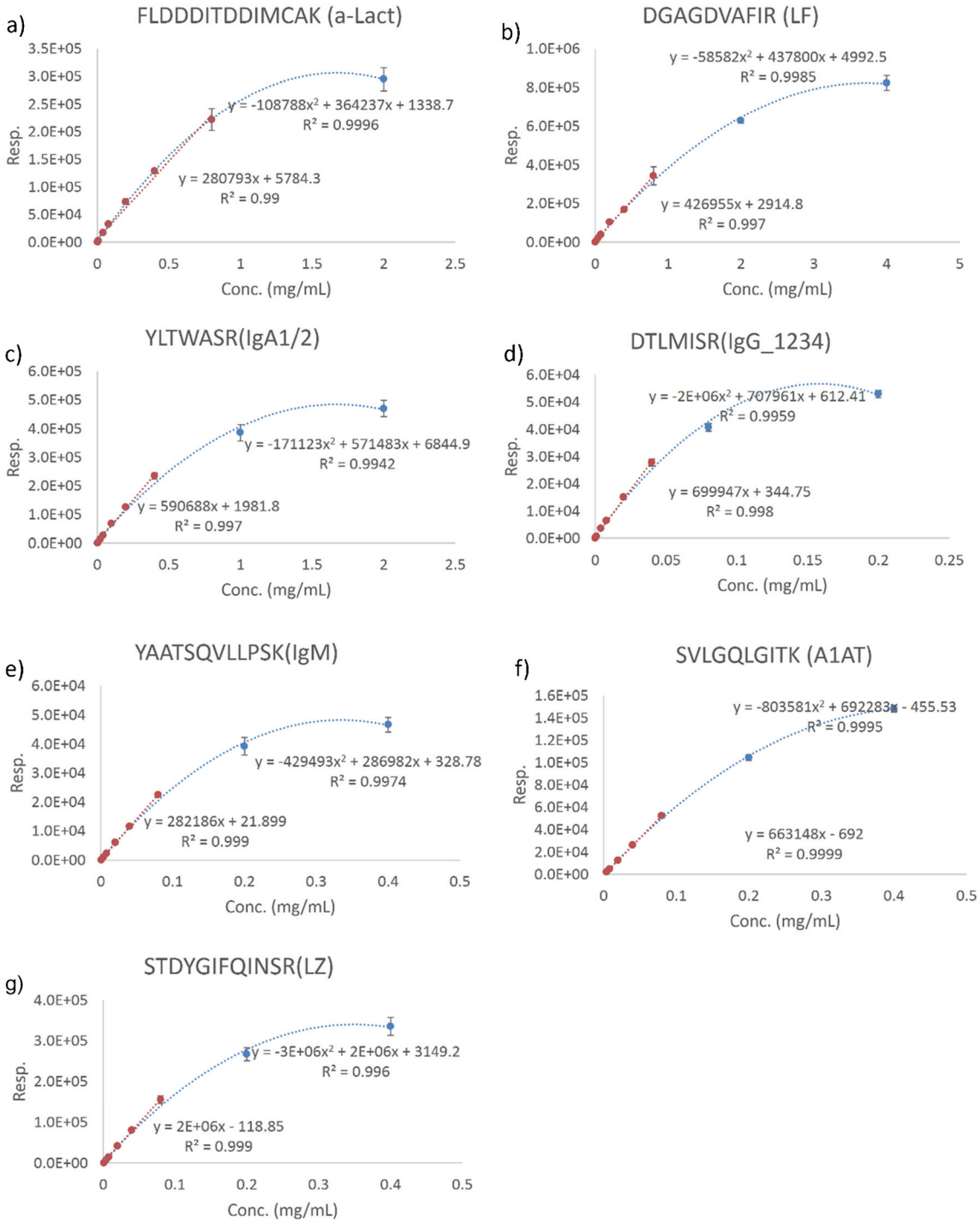

Fig. 4 Peptide calibration curves for protein quantitation. **a** α-lact, **b** LF, **c** IgA1/2, **d** IgG1234, **e** IgM, **f** A1AT, and **g** LZ. The response can be fitted to a quadratic equation (*dashed in blue*). The dynamic rang was over 1000. The linear fit (*dashed in red*) generated an equation with R^2 from 0.99 to 0.999. The linear range was more than 100

transitions of human milk digest are shown in ESM Fig. S2a and S2b for the selected peptides and glycopeptides, respectively.

The concentrations of the targeted proteins were calculated from the calibration curves with the mean concentration and intraday reproducibility as shown in Table 2a. Parallel experiments were performed on two other days to determine the interday reproducibility (Table 2a). High reproducibility of protein quantitation in human milk was obtained with less than 10 % RSD from intraday analysis and slightly higher from interday analysis. The concentrations of the seven proteins from three mature milk samples α-Lact (3.1 ± 0.4 g/L),

Table 2 Quantitation of proteins and their glycoforms. a) Protein concentration (g/L) from three milk samples (A, B, and C). The concentration is representative of the average of the two peptides from each protein except for LZ. RSD is performed on triplicates on the same day (intraday) and different days (interday) to evaluate the reproducibility of the monitored peptides. b) Normalized glycopeptides level from three milk samples and the variation (RSD) from the digestion performed on different days.

a)

	A				B				C			
	Intra day		Inter day		Intra day		Inter day		Intra day		Inter day	
	Mean (g/L)	RSD %	Mean (g/L)	RSD %	Mean (g/L)	RSD %	Mean (g/L)	RSD %	Mean (g/L)	RSD %	Mean (g/L)	*s*
A-Lact	3.65	3.9	3.72	5.2	2.85	1	2.89	7.7	2.78	2.5	2.75	8.9
LF	1.59	6.3	1.58	11	2.8	1.7	2.8	2.3	2.14	1	2.08	5.1
IgA	0.23	5.1	0.22	5	0.61	3.2	0.59	4.8	0.32	3.8	0.31	6.3
IgG	0.047	1	0.045	9	0.02	3	0.019	5.2	0.069	3.3	0.07	5.6
IgM	0.019	4.4	0.02	11.6	0.011	8.1	0.01	7.8	0.028	4.9	0.027	8.8
A1AT	0.016	3.5	0.017	3.8	0.041	2.9	0.04	4.3	0.053	3.9	0.052	4.6
LZ	0.35	2	0.35	6.4	0.032	3.8	0.03	4.9	0.28	2.6	0.27	4.1

b)

		A		B		C	
Protein	Glycopeptide	Log 10 (Glycopeptide abundance/protein abundance)	RSD %	Log 10 (Glycopeptide abundance/protein abundance)	RSD %	Log 10 (Glycopeptide abundance/protein abundance)	RSD %
A1AT	AT-107 H5N4F1S2	–	–	–	–	–	–
A1AT	AT-107 H5N4S2	−1.38	8.1	−1.11	3.3	−1.92	11.1
A1AT	AT-107 H6N5F1S3	–	–	–	–	–	–
A1AT	AT-107 H6N5S3	−1.96	2.8	−2.10	9.2	−1.48	5.8
A1AT	AT-107 H7N6F2S3	–	–	–	–	–	–
A1AT	AT-271 H4N3S1	–	–	–	–	–	–
A1AT	AT-271 H5N4F1S2	–	–	–	–	–	–
A1AT	AT-271 H5N4S1	−2.70	1.1	–	–	–	–
A1AT	AT-271 H5N4S2	−0.89	5.3	−1.70	9.7	−1.65	1.5
A1AT	AT-271 H5N4S2 missed cleavage site	−1.26	1.2	−1.80	3.6	−1.80	7.2
AT	AT-271 H6N5S3	–	–	–	–	–	–
IGA	IGA-131/144 H3N3	–	–	–	–	–	–
IGA	IGA-131/144 H3N4	−1.48	6.3	−1.34	1.3	−1.36	9.6
IGA	IGA-131/144 H3N5F1	–	–	–	–	–	–
IGA	IGA-131/144 H4N4S1	−1.87	2.1	−1.96	6.1	−2.15	13.1
IGA	IGA-131/144 H4N5	−1.43	4.2	−1.74	6.3	−1.39	10.3
IGA	IGA-131/144 H4N5S1	−1.14	2.3	−2.09	9.1	−1.46	1.2
IGA	IGA-131/144 H5F4S1	−2.01	7.9	−2.12	3.2	−2.09	1.3
IGA	IGA-131/144 H5N2	−1.62	9.1	−1.52	11.2	−1.39	5.6
IGA	IGA-131/144 H5N3S1	−2.35	6.1	−2.66	10.2	−2.08	3.7
IGA	IGA-131/144 H5N4	−1.72	6.3	−1.64	11.2	−1.70	8.3
IGA	IGA-131/144 H5N4S2	−2.03	3.5	−2.44	8.3	−2.01	5.9
IGA	IGA-131/144 H5N5S1	−2.08	4.9	−2.60	6.7	−2.07	7.3
IGA	IGA-131/144 H5N5S2	−2.39	3.1	−2.20	11.3	−2.68	8.4
IGA	IGA-131/144 H8N2	−2.14	13.1	−1.89	5.3	−2	7.2
IGA	IGA-131/144 H9N2	-	-	-	-	-	-
IGA	IGA2-205 H3N5F1	−1.38	8.1	−0.95	5.1	−1.00	3.6
IGA	IGA2-205 H5N4F1S1	–	–	–	–	–	–
IGA	IGA2-205 H5N5F1	−0.92	7.8	−1.09	18.1	−1.57	11.2
IGA	IGA2-205 H5N5F1S1	−0.95	5.9	−1.20	12.8	−2	9.5
IGG	IGG H3N4F1_1	−0.42	10.1	−0.86	14.1	−0.22	4.4
IGG	IGG H3N5F1_1	–	–	–	–	–	–

Table 2 (continued)

IGG	IGG H3N5F1_2	−0.92	1.1	−1.03	2.6	−1.06	5.1
IGG	IGG H3N5F1_3_4	0.09	18.2	−0.24	6.3	−0.06	12.1
IGG	IGG H4H5_2	−0.29	9.2	−0.52	5.1	−0.75	6.8
IGG	IGG H4N4_1	–	–	–	–	–	–
IGG	IGG H4N4_2	–	–	–	–	–	–
IGG	IGG H4N4F1_1	−0.26	5.1	−0.68	1.2	−0.11	5.9
IGG	IGG H4N4F1_2	−0.90	3.2	−1.04	4.1	−0.95	1.2
IGG	IGG H4N4F1_3_4	–	–	–	–	–	–
IGG	IGG H4N4F1S1_1	–	–	–	–	–	–
IGG	IGG H4N4F1S1_2	−0.40	5.3	−0.48	8.7	−0.90	8.24
IGG	IGG H4N4F1S1_3_4	–	–	–	–	–	–
IGG	IGG H4N5_1	−0.67	1.1	−1.05	7	−0.34	0.2
IGG	IGG H4N5F1_1	−0.47	5.5	−0.74	8.5	−0.71	3.2
IGG	IGG H4N5F1_2	−0.75	2.1	−0.77	4.1	−1.29	12.1
IGG	IGG H4N5F1_3_4	–	–	–	–	–	–
IGG	IGG H5N4_1	−0.47	15.5	−0.83	11.8	−0.34	2
IGG	IGG H5N4F1_1	–	–	–	–	–	–
IGG	IGG H5N4F1_2	−0.42	7.6	−0.14	1.3	−0.91	2.1
IGG	IGG H5N4F1S1_1	–	–	–	–	–	–
IGG	IGG H5N4F1S1_2	–	–	–	–	–	–
IGG	IGG H5N4F1S1_3_4	–	–	–	–	–	–
IGG	IGG H5N5F1_1	–	–	–	–	–	–
IGM	IGM-209 H4N5F1S1	–	–	–	–	–	–
IGM	IGM-209 H5N4F1S2	–	–	–	–	–	–
IGM	IGM-209 H5N4F1S1	–	–	–	–	–	–
IGM	IGM-209 H5N5F1S1	–	–	–	–	–	–
IGM	IGM-209 H5N5F1S2	–	–	–	–	–	–
IGM	IGM-439 H6N2	−2.23	12.3	−2.36	8.9	−2.47	5.9
IGM	IGM-439 H5N2	–	–	–	–	–	–
IGM	IGM-439 H7N2	–	–	–	–	–	1.1
IGM	IGM-439 H8N2	−2.48	8.1	–	–	–	–
IGM	IGM-439 H9N2	–	–	–	–	–	–
IGM	IGM-46 H5N4F1S1	–	–	–	–	–	–
J	J H4N5	−1.91	7.1	−2.29	7.9	−2.10	4.7
J	J H4N5F1	–	–	–	–	–	–
J	J H5N3F1	−2.09	19.2	−2.22	3.2	−2.05	8.3
J	J H5N3F1S1	–	–	–	–	–	–
J	J H5N4	–	–	–	–	–	–
J	J H5N4F1S1	−1.04	1.5	−1.17	2.1	−1.54	1.9
J	J H5N4F1S2	–	–	–	–	–	–
J	J H5N4S1	–	–	–	–	–	–
LF	LF-156 H5N4F1	−2.54	15.4	−2.43	10	−2.82	12.1
LF	LF-156 H5N4F1S1	−1.77	9.7	−1.54	10	−2.12	1.9
LF	LF-156 H5N4F1S2	−2.13	5.8	−2.19	13.3	−2.62	11.9
LF	LF-156 H5N4F2	−2.12	7.6	−2.54	13	−2.33	11.2
LF	LF-156 H5N4F2S1	−1.32	5	−1.64	10	−1.48	4.7
LF	LF-156 H5N4F3S1	-	-	−3.00	3.1	–	–
LF	LF-156 H6N5F2S1	−2.20	1	−2.72	8.7	−2.60	8.2
LF	LF-156 H6N5F3S1	−2.85	10	−2.77	12.7	−2.62	3.9
LF	LF-497 H5N4F1	−3.00	7.9	−3.10	15.2	−1.89	7.8
LF	LF-497 H5N4F1S1	−1.37	8.2	−1.43	7.8	−1.72	5.3
LF	LF-497 H5N4F1S2	−1.91	5.4	−2.14	6.6	−2.66	3.4
LF	LF-497 H5N4S1	−2.12	9	−1.91	10.3	−2.08	6.3
SC	SC-135 H5N4F1S2	−1.96	8.1	−1.82	7.3	−1.80	4.4
SC	SC-135 H6N6	-	-	-	-	-	-
SC	SC-135 H6N7	−2.52	12.1	−1.55	11.2	−1.96	6.6
SC	SC-135 H7N6	–	–	–	–	–	–
SC	SC-135 H7N7	–	–	–	–	–	–
SC	SC-186 H6N6S1	–	–	–	–	–	–
SC	SC-421 H5N4F1S1	−1.72	8.1	−0.94	1.2	−1.89	8.7
SC	SC-469 H3N5	–	–	–	–	–	–
SC	SC-469 H4N5F1	−1.96	2.4	−1.35	8.7	−1.96	5.1
SC	SC-469 H5N2	–	–	–	–	–	–
SC	SC-469 H5N4F1S1	−1.08	10.4	−1.00	3.1	−1.43	10.2

Table 2 (continued)

SC	SC-469 H5N4F1S2	−2.29	15.3	−1.66	11.2	−1.89	7.7
SC	SC-469 H6N2	−2.29	3.8	−1.96	3.3	−2.15	4.8
SC	SC-499 H4N5F1S1	–	–	–	–	–	–
SC	SC-499 H5N5F1S1	−1.72	2.3	−1.85	8.1	−1.82	4
SC	SC-499 H5N5F1S2	−1.70	4.5	−1.49	7.1	−1.92	6.8

Any glycopeptide with S/N less than 10 was shown as "–"

H hexose, *N* HexNAc, *F* fucose, *S*, *N*-acetyl neuraminic acid

LF (2.2 ± 0.5 g/L), IgA (0.39 ± 0.12 g/L), IgG (0.045 ± 0.02 g/L), IgM (0.019 ± 0.007 g/L), A1AT (0.037 ± 0.015 g/L), and LZ (0.22 ± 0.13 g/L) include biological variations from the three individuals.

Conventional methods including radial immunodiffusion, immunoelectrophoresis, enzyme-linked immunosorbent assay (ELISA), sodium dodecyl sulfate polyacrylamide gel electrophoresis (SDS-PAGE), and microparticle-enhanced nephelometric immunoassay were the commonly used analytical methods to quantitate individual proteins in human milk [6, 28, 29, 67–69]. Previous studies have shown similar concentrations of these proteins using other techniques [65, 67–69]. However, none of these methods monitor protein glycosylation. Here, we present for the first time, a mass spectrometric method to quantify seven proteins along with their glycoforms in human milk.

The approach we developed takes protein abundances into consideration. Quantitation of glycosylation in milk proteins, where the vast majority of studies have been performed, is currently limited only to the ion abundances of glycans/glycopeptides [70, 71]. However, there has been no information on how the protein level affects measured glycan abundances. We have previously reported a method for IgG where the glycopeptide signals were normalized to the protein abundances to remove the contribution of protein concentration [36]. Here, we expand this capability for several proteins in milk. For LF, IgM, and A1AT, the glycopeptide signals were normalized to the peptide yielding the higher ion abundance. For sIgA and IgG, because of their complexity with different polypeptides and subclasses, the glycopeptides were normalized to respective peptides on SC, IgA1, IgA2, J chain, IgG1, IgG2, and IgG3/4. The unique peptide from these polypeptides that were monitored are listed in Table 1a. Glycopeptides from IgA1 (^{144}N) and IgA2 (^{131}N) could not be distinguished because the tryptic peptides are identical; thus, the signals were normalized to the common peptide from IgA1/2. Similarly, glycopeptides from IgG3 and IgG4 could not be distinguished; thus, the signals were normalized to the sum of the two peptides from IgG3 and IgG4. The normalized glycopeptide level from the three milk samples with their RSD is shown in Table 2b. A relatively higher RSD was observed for glycopeptides, which is expected. The variation is likely due to the incomplete trypsin digestion due to the presence of glycan [72–74] that may block the cleavage site. Some of the glycopeptides were not quantified due to their low S/N (<10) (Table 2b). Because the concentration of these

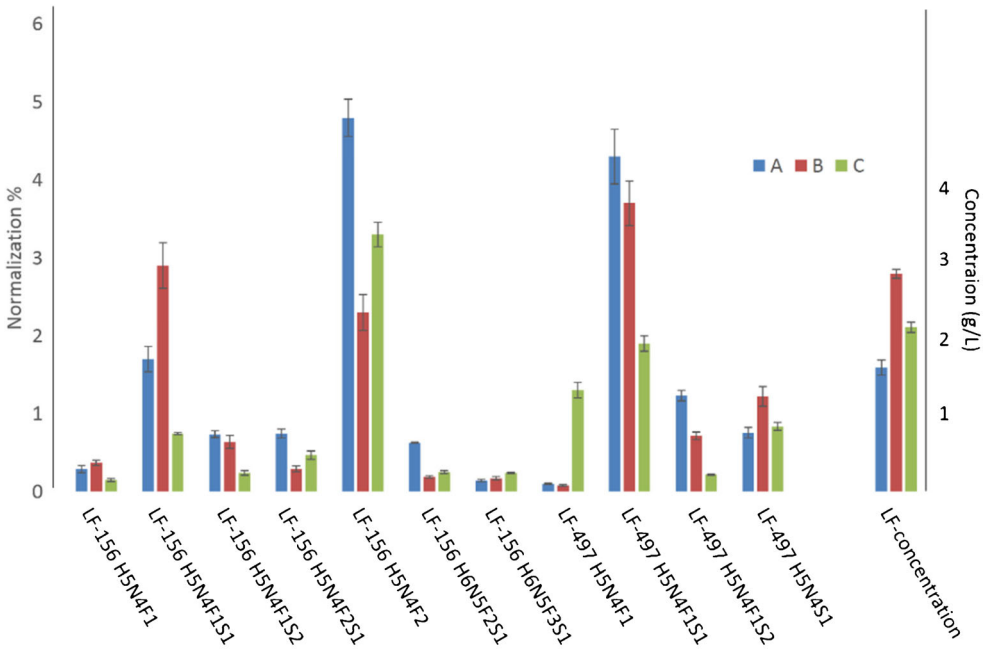

Fig. 5 Eleven normalized LF glycopeptide abundances monitored from three milk samples (**a**, **b**, and **c**). LF concentration (g/L) of three milk samples on the right of the plot. Normalization was performed with the ratio between glycopeptide signal peak area and the LF peptide peak area. This suggests the dynamic variation on site-specific glycosylation. *Error bars* are representative of reproducibility from replicates on different days

proteins in milk usually ranges some three orders of magnitude, signals of glycopeptides from the less abundant proteins such as IgG and IgM were limited. However, quantitation of these glycopeptides could be achieved alternatively by the enrichment of the respective glycoproteins.

Differences in levels of glycosylation were observed from the three milk samples. For example, in Fig. 5, the 11 observed LF-glycopeptides are provided along with the concentration of LF. There appears to be no correlation between glycosylation and protein concentrations. However, the method illustrates well the quantitation of protein and their site-specific glycosylation simultaneously, and it will facilitate the understanding of function of glycosylation in human milk.

Conclusion

We have established an analytical method using MRM for the quantitation of milk proteins and their glycoforms in a rapid throughput manner. The approach detailed here provides quantitative analyses of proteins and the site-specific glycosylation. Quantitative glycosylation information at a given site is obtained by normalization to the protein measured abundances, which was previously not feasible. High sensitivity and reproducibility were observed from this MRM analysis. The method developed in this study is currently being used to analyze large sample sets and will aid in elucidating the biological functions of human milk glycoproteins during lactation.

Acknowledgments We are grateful for funds from the National Institutes of Health (GM049077, HD061923, P42 ES02710, R01AT007079, and HD059127) and California Dairy Research Foundation Grant 06 LEC-01-NH. The Agilent QTOF MS instrument was obtained through a grant (S10RR027639).

Compliance with ethical standards

Conflict of interest The authors declare that there is no conflict of interest.

Informed consent Informed consents were obtained from all individual participants.

Human and animal rights All the procedures related to human samples were performed in accordance with policies, procedures, and regulations approved by the ethics committee at the University of California in Davis.

References

1. Lee H, Lerno LA, Choe Y, Chu CS, Gillies LA, Grimm R, et al. Multiple precursor ion scanning of gangliosides and sulfatides with a reversed-phase microfluidic chip and quadrupole time-of-flight mass spectrometry. Anal Chem. 2012;84(14):5905–12. doi:10.1021/ac300254d.
2. Ruhaak LR, Lebrilla CB. Advances in analysis of human milk oligosaccharides. Adv Nutr. 2012;3(3):406S–14. doi:10.3945/an.112.001883.
3. Totten SM, Zivkovic AM, Wu S, Ngyuen U, Freeman SL, Ruhaak LR, et al. Comprehensive profiles of human milk oligosaccharides yield highly sensitive and specific markers for determining secretor status in lactating mothers. J Proteome Res. 2012;11(12):6124–33. doi:10.1021/pr300769g.
4. Lönnerdal B. Bioactive proteins in human milk: mechanisms of action. J Pediatr. 2010;156(2):S26–30.
5. Dallas DC, Guerrero A, Khaldi N, Castillo PA, Martin WF, Smilowitz JT, et al. Extensive in vivo human milk peptidomics reveals specific proteolysis yielding protective antimicrobial peptides. J Proteome Res. 2013;12(5):2295–304.
6. Froehlich JW, Dodds ED, Barboza M, McJimpsey EL, Seipert RR, Francis J, et al. Glycoprotein expression in human milk during lactation. J Agric Food Chem. 2010;58(10):6440–8.
7. Barboza M, Pinzon J, Wickramasinghe S, Froehlich JW, Moeller I, Smilowitz JT, et al. Glycosylation of human milk lactoferrin exhibits dynamic changes during early lactation enhancing its role in pathogenic bacteria-host interactions. Mol Cell Proteomics. 2012;11(6).
8. Liao Y, Jiang R, Lönnerdal B. Biochemical and molecular impacts of lactoferrin on small intestinal growth and development during early life11 This article is part of a Special Issue entitled Lactoferrin and has undergone the Journal's usual peer review process. Biochem Cell Biol. 2012;90(3):476–84. doi:10.1139/o11-075.
9. Lönnerdal B. Nutritional and physiologic significance of human milk proteins. Am J Clin Nutr. 2003;77(6):1537S–43.
10. Zivkovic AM, German JB, Lebrilla CB, Mills DA. Human milk glycobiome and its impact on the infant gastrointestinal microbiota. Proc Natl Acad Sci. 2011;108(Supplement 1):4653–8.
11. Lasky LA. Selectins: interpreters of cell-specific carbohydrate information during inflammation. Science. 1992;258(5084):964–9.
12. Lowe JB. Glycosyltransferases and glycan structures contributing to the adhesive activities of L-, E-and P-selectin counter-receptors. In: Biochemical Society Symposia, 2002. London; Portland on behalf of The Biochemical Society; 1999, pp 33–46
13. Fukuda MN, Sasaki H, Lopez L, Fukuda M. Survival of recombinant erythropoietin in the circulation: the role of carbohydrates. Blood. 1989;73(1):84–9.
14. Shental-Bechor D, Levy Y. Folding of glycoproteins: toward understanding the biophysics of the glycosylation code. Curr Opin Struct Biol. 2009;19(5):524–33.
15. Pellegrini A, Thomas U, Bramaz N, Hunziker P, von Fellenberg R. Isolation and identification of three bactericidal domains in the bovine α-lactalbumin molecule. Biochim Biophys Acta (BBA) Gen Subj. 1999;1426(3):439–48.
16. Ebner K, Brodbeck U. Biological role of α−lactalbumin: a review. J Dairy Sci. 1968;51(3):317–22.
17. Norderhaug I, Johansen F, Schjerven H, Brandtzaeg P. Regulation of the formation and external transport of secretory immunoglobulins. Crit Rev Immunol. 1999;19(5–6):481–508.
18. Royle L, Roos A, Harvey DJ, Wormald MR, Van Gijlswijk-Janssen D, Redwan E-RM, et al. Secretory IgA N-and O-glycans provide a link between the innate and adaptive immune systems. J Biol Chem. 2003;278(22):20140–53.
19. Wold AE, Mestecky J, Tomana M, Kobata A, Ohbayashi H, Endo T, et al. Secretory immunoglobulin A carries oligosaccharide receptors for Escherichia coli type 1 fimbrial lectin. Infect Immun. 1990;58(9):3073–7.
20. Zauner G, Selman MH, Bondt A, Rombouts Y, Blank D, Deelder AM, et al. Glycoproteomic analysis of antibodies. Mol Cell Proteomics. 2013;12(4):856–65.

21. Chowanadisai W, Lönnerdal B. α1-Antitrypsin and antichymotrypsin in human milk: origin, concentrations, and stability. Am J Clin Nutr. 2002;76(4):828–33.
22. Lonnerdal B. Bioactive proteins in human milk: mechanisms of action. (1097–6833 (Electronic))
23. Newburg DS, Walker WA. Protection of the neonate by the innate immune system of developing gut and of human milk. Pediatr Res. 2007;61(1):2–8.
24. Ng-Kwai-Hang K, Kroeker E. Rapid separation and quantification of major caseins and whey proteins of bovine milk by polyacrylamide gel electrophoresis. J Dairy Sci. 1984;67(12):3052–6.
25. Kinghorn NM, Norris CS, Paterson GR, Otter DE. Comparison of capillary electrophoresis with traditional methods to analyse bovine whey proteins. J Chromatogr A. 1995;700(1):111–23.
26. Palmano KP, Elgar DF. Detection and quantitation of lactoferrin in bovine whey samples by reversed-phase high-performance liquid chromatography on polystyrene–divinylbenzene. J Chromatogr A. 2002;947(2):307–11.
27. Hurley IP, Coleman RC, Ireland HE, Williams JH. Use of sandwich IgG ELISA for the detection and quantification of adulteration of milk and soft cheese. Int Dairy J. 2006;16(7):805–12.
28. Montagne PM, Trégoat VS, Cuillière ML, Béné MC, Faure GC. Measurement of nine human milk proteins by nephelometric immunoassays: application to the determination of mature milk protein profile. Clin Biochem. 2000;33(3):181–6.
29. Montagne P, Cuillière ML, Molé C, Béné MC, Faure G. Microparticle-enhanced nephelometric immunoassay of lysozyme in milk and other human body fluids. Clin Chem. 1998;44(8):1610–5.
30. Kuzyk MA, Smith D, Yang J, Cross TJ, Jackson AM, Hardie DB, et al. Multiple reaction monitoring-based, multiplexed, absolute quantitation of 45 proteins in human plasma. Mol Cell Proteomics. 2009;8(8):1860–77.
31. Anderson L, Hunter CL. Quantitative mass spectrometric multiple reaction monitoring assays for major plasma proteins. Mol Cell Proteomics. 2006;5(4):573–88.
32. Keshishian H, Addona T, Burgess M, Kuhn E, Carr SA. Quantitative, multiplexed assays for low abundance proteins in plasma by targeted mass spectrometry and stable isotope dilution. Mol Cell Proteomics. 2007;6(12):2212–29.
33. Affolter M, Grass L, Vanrobaeys F, Casado B, Kussmann M. Qualitative and quantitative profiling of the bovine milk fat globule membrane proteome. J Proteome. 2010;73(6):1079–88.
34. Shi T, Su D, Liu T, Tang K, Camp DG, Qian WJ, et al. Advancing the sensitivity of selected reaction monitoring-based targeted quantitative proteomics. Proteomics. 2012;12(8):1074–92.
35. Zhang J, Lai S, Zhang Y, Huang B, Li D, Ren Y. Multiple reaction monitoring-based determination of bovine α-lactalbumin in infant formulas and whey protein concentrates by ultra-high performance liquid chromatography–tandem mass spectrometry using tryptic signature peptides and synthetic peptide standards. Anal Chim Acta. 2012;727:47–53.
36. Hong Q, Lebrilla CB, Miyamoto S, Ruhaak LR. Absolute quantitation of immunoglobulin G and its glycoforms using multiple reaction monitoring. Anal Chem. 2013;85(18):8585–93. doi:10.1021/ac4009995.
37. Nwosu CC, Seipert RR, Strum JS, Hua SS, An HJ, Zivkovic AM, et al. Simultaneous and extensive site-specific N-and O-glycosylation analysis in protein mixtures. J Proteome Res. 2011;10(5):2612–24.
38. Huang J, Lee H, Zivkovic AM, Smilowitz JT, Rivera N, German JB, et al. Glycomic analysis of high density lipoprotein shows a highly sialylated particle. J Proteome Res. 2014;13(2):681–91. doi:10.1021/pr4012393.
39. Baker HM, Baker EN. Lactoferrin and iron: structural and dynamic aspects of binding and release. Biometals. 2004;17(3):209–16.
40. Haridas M, Anderson B, Baker E. Structure of human diferric lactoferrin refined at 2.2 A resolution. Acta Crystallogr D Biol Crystallogr. 1995;51(5):629–46.
41. Legrand D. Lactoferrin, a key molecule in immune and inflammatory processes11. This article is part of Special Issue entitled Lactoferrin and has undergone the Journal's usual peer review process. Biochem Cell Biol. 2011;90(3):252–68. doi:10.1139/o11-056.
42. Liao Y, Alvarado R, Phinney B, Lonnerdal B. Proteomic characterization of human milk whey proteins during a twelve-month lactation period. J Proteome Res. 2011;10(4):1746–54. doi:10.1021/pr101028k.
43. Blanchard H, Yu X, Coulson BS, von Itzstein M. Insight into host cell carbohydrate-recognition by human and porcine rotavirus from crystal structures of the virion spike associated carbohydrate-binding domain (VP8*). J Mol Biol. 2007;367(4):1215–26.
44. Sela DA, Li Y, Lerno L, Wu S, Marcobal AM, German JB, et al. An infant-associated bacterial commensal utilizes breast milk sialyloligosaccharides. J Biol Chem. 2011; 286(14). doi:10.1074/jbc.M110.193359
45. Pyburn TM, Bensing BA, Xiong YQ, Melancon BJ, Tomasiak TM, Ward NJ, et al. A structural model for binding of the serine-rich repeat adhesin GspB to host carbohydrate receptors. PLoS Pathog. 2011;7(7), e1002112.
46. Viswanathan K, Chandrasekaran A, Srinivasan A, Raman R, Sasisekharan V, Sasisekharan R. Glycans as receptors for influenza pathogenesis. Glycoconj J. 2010;27(6):561–70.
47. Varki A. Glycan-based interactions involving vertebrate sialic-acid-recognizing proteins. Nature. 2007;446(7139):1023–9.
48. Wuhrer M, Stam JC, van de Geijn FE, Koeleman CA, Verrips CT, Dolhain RJ, et al. Glycosylation profiling of immunoglobulin G (IgG) subclasses from human serum. Proteomics. 2007;7(22):4070–81.
49. Ruhaak LR, Uh H-W, Beekman M, Koeleman CA, Hokke CH, Westendorp RG, et al. Decreased levels of bisecting GlcNAc glycoforms of IgG are associated with human longevity. PLoS One. 2010;5(9), e12566.
50. Arnold JN, Wormald MR, Suter DM, Radcliffe CM, Harvey DJ, Dwek RA, et al. Human serum IgM glycosylation identification of glycoforms that can bind to mannan-binding lectin. J Biol Chem. 2005;280(32):29080–7.
51. Chapman A, Kornfeld R. Structure of the high mannose oligosaccharides of a human IgM myeloma protein. I. The major oligosaccharides of the two high mannose glycopeptides. J Biol Chem. 1979;254(3):816–23.
52. Chapman A, Kornfeld R. Structure of the high mannose oligosaccharides of a human IgM myeloma protein. II. The minor oligosaccharides of high mannose glycopeptide. J Biol Chem. 1979;254(3):824–8.
53. Carrell RW, Jeppsson J-O, Laurell C-B, Brennan SO, Owen MC, Vaughan L, et al. Structure and variation of human alpha 1-antitrypsin. Nature. 1982;298(5872):329–34.
54. Gettins PG. Serpin structure, mechanism, and function. Chem Rev. 2002;102(12):4751–804.
55. Sarkar A, Wintrode PL. Effects of glycosylation on the stability and flexibility of a metastable protein: the human serpin α 1 −antitrypsin. Int J Mass Spectrom. 2011;302(1):69–75.
56. Kwon K-S, Kim J, Shin HS, Yu M-H. Single amino acid substitutions of alpha 1-antitrypsin that confer enhancement in thermal stability. J Biol Chem. 1994;269(13):9627–31.
57. Carrell R, Jeppsson J-O, Vaughan L, Brennan S, Owen M, Boswell D. Human α 1−antitrypsin: carbohydrate attachment and sequence homology. FEBS Lett. 1981;135(2):301–3.
58. Kolarich D, Turecek PL, Weber A, Mitterer A, Graninger M, Matthiessen P, et al. Biochemical, molecular characterization, and glycoproteomic analyses of α1-proteinase inhibitor products used for replacement therapy*. Transfusion. 2006;46(11):1959–77.

59. Kolarich D, Weber A, Turecek PL, Schwarz HP, Altmann F. Comprehensive glyco-proteomic analysis of human α1-antitrypsin and its charge isoforms. Proteomics. 2006;6(11):3369–80.
60. Woof JM, Kerr MA. IgA function–variations on a theme. Immunology. 2004;113(2):175–7.
61. Kerr M. The structure and function of human IgA. Biochem J. 1990;271(2):285.
62. Rebecchi KR, Wenke JL, Go EP, Desaire H. Label-free quantitation: a new glycoproteomics approach. J Am Soc Mass Spectrom. 2009;20(6):1048–59.
63. Roth Z, Yehezkel G, Khalaila I. Identification and quantification of protein glycosylation. Int J Carbohydrate Chem. 2012
64. Stavenhagen K, Hinneburg H, Thaysen-Andersen M, Hartmann L, Silva DV, Fuchser J, et al. Quantitative mapping of glycoprotein micro-heterogeneity and macro-heterogeneity: an evaluation of mass spectrometry signal strengths using synthetic peptides and glycopeptides. J Mass Spectrom. 2013;48(6):627–39.
65. Räihä NC. Nutritional proteins in milk and the protein requirement of normal infants. Pediatrics. 1985;75(1):136–41.
66. Hambraeus L, Lönnerdal B, Forsum E, Gebre-Medhin M. Nitrogen and protein components of human milk. Acta Paediatr. 1978;67(5):561–5.
67. Cuillière M-L, Abbadi M, Molé C, Montagne P, Béné M-C, Faure G. Microparticle-enhanced nephelometric immunoassay of alpha-lactalbumin in human milk. J Immunoass Immunochem. 1997;18(1):97–109.
68. Koenig Á, de Albuquerque Diniz EM, Barbosa SFC, Vaz FAC. Immunologic factors in human milk: the effects of gestational age and pasteurization. J Hum Lact. 2005;21(4):439–43.
69. Rai D, Adelman AS, Zhuang W, Rai GP, Boettcher J, Lönnerdal B. Longitudinal changes in lactoferrin concentrations in human milk—a global systematic review. Crit Rev Food Sci Nutr. (just-accepted) 2013.
70. Smilowitz JT, Totten SM, Huang J, Grapov D, Durham HA, Lammi-Keefe CJ, et al. Human milk secretory immunoglobulin A and lactoferrin N-glycans are altered in women with gestational diabetes mellitus. J Nutr. 2013;143(12):1906–12.
71. Nwosu CC, Aldredge DL, Lee H, Lerno LA, Zivkovic AM, German JB, et al. Comparison of the human and bovine milk N-glycome via high-performance microfluidic chip liquid chromatography and tandem mass spectrometry. J Proteome Res. 2012;11(5):2912–24.
72. Bezouška K, Sklenář J, Novák P, Halada P, Havlíček V, Kraus M, et al. Determination of the complete covalent structure of the major glycoform of DQH sperm surface protein, a novel trypsin-resistant boar seminal plasma O-glycoprotein related to pB1 protein. Protein Sci. 1999;8(7):1551–6.
73. Cauchi MR, Henchal E, Wright PJ. The sensitivity of cell-associated dengue virus proteins to trypsin and the detection of trypsin-resistant fragments of the nonstructural glycoprotein NS1. Virology. 1991;180(2):659–67.
74. Loo TW, Clarke DM. The human multidrug resistance P-glycoprotein is inactive when its maturation is inhibited: potential for a role in cancer chemotherapy. FASEB J. 1999;13(13):1724–32.